TURBULENCE MODELS IN PREDICTING FLOW STRUCTURE AROUND AN ABSTACLE IN VICINITY OF A FLAT PLATE

M. Kahrom , A. Heydari†

Ferdowsi University of Mashhad

Faculty of Engineering of Ferdowsi University of Mashhad

mohsen.kahrom@yahoo.co.uk

†Islamic Azad University of semnan branch

Faculty of Engineering of Islamic Azad University of semnan

heydary.a@gmail.com

Abstract. *Flow structure around an obstacle in vicinity of a flat plate is analyzed. Within the experience, the stream of velocity parallel to a flat plate flowing at 22m/s was assumed. A square rod as an insert is placed inside a turbulent boundary layer at the vicinity of the flat plate. The distance of the square insert from the wall is then changed to measure the effect of its position on boundary layer behavior near the wall. The insert divides the flow into two parts. The lower part washes away the thin remaining boundary layer on the plat away, while the second part of the flow jumps upon the top side of the insert, forming the wake zone at the downstream to the obstacle. Both parts at downstream interact on each other and produce a complex flow structure which is the main task of the present paper to study its performance. The flow structure is highly dependent on the distance of obstacle from the flat plate. Experimental measurements together with computational simulation are concurrently employed to get an insight to the flow formation. In the numerical simulations, the two equations K-ε and K-ω turbulence models together with the one equation Spalart-Allmaras are used to predict the flow structure and boundary layer characteristics. The square obstacle is moved step by step away from the flat plate and in each step the velocity distribution is measured in a wind tunnel and simultaneously by computation. The measuring sections are arranged at different stations from the obstacle, down to a point at downstream at which disturbances die away. The oscillatory solutions due to the existence of vortices were noticed. To gain the averaged values of the velocity, as is the case for hot wire measurements as well, averaging of the velocities over a period of oscillation was employed. Finally comparison between numerical evaluation and experimental solutions is made and flow structure near the wall is discussed.*

Key words: Square Obstacle, Vicinity of a Flat Plate, K-ε, K-ω, Spalart-Allmaras

1 INTRODUCTION

A wall jet is defined as a jet bounded on one side by a wall. In practice, the wall jets form when a flow of a film cooling sweeps upon a gas turbine blade, or ventilating flow is touching one of the side walls of a room and more interesting for authors of present paper, when a turbulent boundary layer is disturbed by a cylinder.

Turbulent wall jets have many practical uses and have attracted the attention of many experimentalists. There have been many attempts to find scaling laws for these flows, i.e., to find dimensionless coordinates in which the velocity distributions for the various cross-sections collapse to a single curve. We find that wall jet flows consist of two self-similar layers: a top layer and a wall layer, separated by a mixing layer where the velocity is close to the maximum. Studies on the problems of wake development and vortex shedding behind a rectangular cylinder in free-stream flows have recently been investigated both numerically and experimentally by Davis and Moore [3], Franke et al. [4], Okajima and Sakai [5] and Patankar and Kelkar [6].

Classical presentation of a wall jet is shown in fig. 1 A. In this figure, the jet enters to a flow field from a slot and forms a velocity field, figure 1 B. Unlike in a free jet, the mixing here is substantially influenced by the walls. The

Scaling laws reads as, [12]: $$\frac{u}{u_{\max}} = f\left(\frac{y}{y_{1/2}}\right)$$

The formula describes the jet structure. The u_{max} is the maximum velocity at a given section x, and $y1/2$ is the coordinate, which also depends on x, where the mean velocity is equal to one half of the maximum velocity; this coordinate has always been taken to be above the point where the maximum velocity is reached, and indeed in the majority of experiments the resolution close to the wall has been insufficient to determine the coordinate under the maximum where one half of the maximum mean velocity is also achieved, though this coordinate obviously exists.

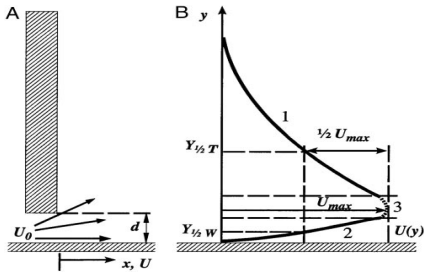

Figure 1: The schematic structure of the wall jet flow. (*A*) The apparatus that produces a wall jet. (*B*) The structure of wall jet flow. 1, top self-similar layer; 2,wall self-similar layer; 3, mixing layer where the velocity is close to maximum.

In practical flow situations may involve obstacles located close to a wall, e.g., flow past a suspension bridge or pipelines near the ground or water surfaces, flow past heat exchanger tubes near walls, etc. The vicinity of a wall can have a distinct influence on the vortex shedding. The influence of the wall is to cause asymmetry in the strength of the vortex sheets. When there is a gap between the cylinder and the wall, the onset of vortex formation appears at a critical gap height. There have been some studies on the effect of wall on vortex shedding behind a square cylinder, e.g., [1–7] and the references therein.

In a general consideration the wall jet is formed of two self-similar layers: a top layer and a wall layer, separated by a mixing layer where the velocity is close to a maximum. However, the main difficulty which stands with the near wall jets is the change of the sign of turbulent stress, τ_t in the outer-layer of the internal jet. In this region, the turbulence production ($\propto \tau_t \frac{\partial \bar{u}}{\partial y}$) turns to be negative. This means that the energy is transferred from the

turbulence fluctuations to the mean motion. This feature of the flow is in contradiction with the eddy viscosity and mixing length modeling assumptions, [Schlechting].

On the other hand, for difficult flows which are developing in vicinity of a wall, hot wire measurements of velocity are erroneous. Other techniques, if available, are very expensive and not always practical. If one is trying to study such a complicated flow field, one way is to measure the flow up to a safe possible point near the wall. If the measurement satisfies solution of a numerical program, then details of the flow can be concluded from the numerical solution. If such an approach to a flow study is accepted, the turbulence model must be selected cautiously. DNS is an obvious accurate choice to study complex flows, but the technique relies upon sophisticated computer facilities, not always available and neither economical. Ahlman et. al. [15] have simulated a plane turbulent wall-jet, using DNS model. The calculation time reported to take 22000 CPU hrs on a Linux computer. LES is much more popular and almost reachable by almost all research persons. Sarkar et.al [7]. employed LES to study flow structure around a circular cylinder at the vicinity of a wall. The cylinder divides the flow into two parts. One forming a jet and the second branch forms a vertical zone. Interaction of these two flow field is then compared to measurments data and reported to be in good agreement. However, EVM's are more popular to research workers and are believed to achieve satisfactory results even in difficult environments. Fashola et.al. [16] employed the standard $k-\varepsilon$ model to predict the effect of main stream turbulence intensity on the heat and skin friction coefficient from a plane wall jet.

Qualitatively, vortex generation around a circular cylinder differs by that of a square cylinder. In the case of a circular cylinder the separation points can slide around the smooth surface, whereas on a square cylinder the separation points are broadly fixed at the corner points, consequently exerting influence on the vortex shedding process ahead of it. The experimental and numerical study on the turbulent flow around a square cylinder placed at various heights above a wall at high Reynolds numbers were carried out by Bosch and Rodi [17]. Through experimental studies, Bosch et al. [18] observed that irregular or intermittent vortex shedding occurs for gap heights just larger than the gap height where complete suppression of vortex shedding occurs. Recently Liou et al. [19] presented a three-dimensional large eddy simulation of the turbulent wake behind a square cylinder. Their result shows that the celerity of the positive vortex shedings from the lower side of the cylinder is smaller than that of the upper side shed vortices. This is due to the interaction of the wall boundary layer. In all the above studies the Reynolds number which is based on the cylinder height were considered to be of order O(104) [1].

2 MODELING

2.1 Experimental Modeling

In this model we have a square obstacle which is in vicinity of a flat plate that is shown in fig.2. This time the separated flow from top of the square affect the wall jet that occurs in bottom of the square. We investigated the effect of obstacle's distance from flat plate (d) on the flow pattern formation in behind of obstacle.

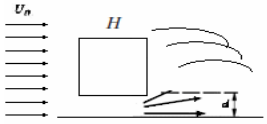

Figure 2: the schematic model of square obstacle in vicinity of a flat plate

Experimental velocity magnitudes were taken in several distances behind the obstacle. Inlet velocity was 23.5 m/s and dimensions of square is 16×16mm. We measured velocity magnitude at 8 sections behind the obstacle. Distance between each section is 16mm. Then we changed obstacle's distance from flat plate (d) up to 9mm and obtained velocity profile in each section of each step. Measurements were done in a wind tunnel with some 1D hot wire in Sabzevar University.

2.2 Numerical Modeling

In this section some numerical simulations are done. We apply some turbulence models to predict flow behavior near wall. The simplest "complete models" of turbulence are two-equation models in which the solution of two separate transport equations allows the turbulent velocity and length scales to be independently determined. Some models that we used in our simulations are k-ε, k-ω. Another one equation model that we used in our comparison is Spalart-Allmaras model.

A non-uniform grid distribution in the computational domain is incorporated (see Fig. 3). The grid is finer near the faces of the square cylinder and plane wall to better resolve the gradients near the solid surfaces.

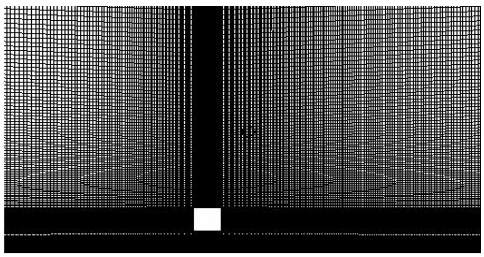

Fig.3. The arrangement of the computational grid in the computational domain.

Time-dependent, two-dimensional Navier–Stokes equations for a constant property fluid in non-dimensional conservative form are given by:

$$\frac{\partial u}{\partial x}+\frac{\partial v}{\partial y}=0$$

$$\frac{\partial u}{\partial t}+\frac{\partial u^2}{\partial x}+\frac{\partial uv}{\partial y}=-\frac{\partial p}{\partial x}+\frac{1}{Re}\left(\frac{\partial^2 u}{\partial x^2}+\frac{\partial^2 u}{\partial y^2}\right)$$

$$\frac{\partial v}{\partial t}+\frac{\partial uv}{\partial x}+\frac{\partial v^2}{\partial y}=-\frac{\partial p}{\partial y}+\frac{1}{Re}\left(\frac{\partial^2 v}{\partial x^2}+\frac{\partial^2 v}{\partial y^2}\right) \qquad (1)$$

At the far upstream, the transverse velocity component is set to zero, and a sheared profile for the longitudinal velocity component is assumed. At the plane wall and cylinder surface, no-slip boundary conditions is applied. u=v=0 on the cylinder and on the plane wall y=0 and Further, u →y, v→0 in the upstream.

2.2.1 The K-ε model

The turbulence kinetic energy k, and its rate of dissipation, ε, are obtained from the following transport equations, [8, and 11]:

$$\frac{\partial \rho \overline{U}\, k}{\partial x}+\frac{\partial \rho \overline{V}\, k}{\partial y}=\frac{\partial}{\partial y}\left[\left(\mu+\frac{\mu_t}{\sigma_k}\right)\frac{\partial k}{\partial y}\right]+\underbrace{\mu_t\underbrace{\left(\frac{\partial \overline{U}}{\partial y}\right)^2}_{term}}_{production}-\underbrace{\rho\frac{k^{\frac{3}{2}}}{l}}_{diss.\,term} \qquad (2)$$

$$\frac{\partial \rho \overline{U}\,\varepsilon}{\partial x}+\frac{\partial \rho \overline{V}\,\varepsilon}{\partial y}=\frac{\partial}{\partial y}\left[\left(\mu+\frac{\mu_t}{\sigma_\varepsilon}\right)\frac{\partial \varepsilon}{\partial y}\right]+\underbrace{c_{\varepsilon 1}\frac{\varepsilon}{k}\mu_t\left(\frac{\partial \overline{U}}{\partial y}\right)^2}_{production\ term}-\underbrace{\rho c_{\varepsilon 2}\frac{\varepsilon^2}{k}}_{diss\ .term} \qquad (3)$$

The turbulent length scale is obtained from:

$$l=\frac{k^{\frac{3}{2}}}{\varepsilon} \qquad (4)$$

The turbulent viscosity is computed from:

$$\mu_t=\rho c_\mu \frac{k^2}{\varepsilon} \qquad (5)$$

Where

$$c_{\varepsilon 1}=c_{\varepsilon 2}-\frac{k^2}{c_\mu^{1/2}\sigma_\varepsilon} \qquad ;c_{\varepsilon 2}=\frac{m+1}{m} \qquad (6)$$

Experimental data give m=1.25±0.06 [1], and $c_{\varepsilon 2}=1.92$ is chosen. The last two constants, σ_k and σ_ε, are optimized by applying the model to various fundamental flows such as flow in channel, pipes, jets, wakes, etc. The five constants are given the following values:

$$c_\mu=0.09,\quad c_{\varepsilon 1}=1.44,\quad c_{\varepsilon 2}=1.92,\quad \sigma_k=1.0,\quad \sigma_\varepsilon=1.31 \qquad (7)$$

2.2.2 The K-ω model

It can be claimed that the ω equation in the standard k-ω model was derived using the more complex method of transforming a K-ε model to a K-ω model. It is however more likely that the simpler route of dimensionally modify the k-equation was used, since the ω model only composes of a production term, a destruction term and the two standard diffusion terms ,[9,10,12](turbulent and viscous respectively).
Thus using method 1, the k equation is multiplied with ω/k to yield the ω equation as:

$$\frac{D\omega}{Dt}=\underbrace{C_{\omega 1}f_\omega}_{\alpha}\frac{\omega}{k}P_k-C_{\omega 2}\omega^2+\frac{\partial}{\partial x_j}\left[\left(\upsilon+\frac{\upsilon_t}{\sigma_\omega}\right)\frac{\partial \omega}{\partial x_j}\right] \qquad (8)$$

Where

$$C_{\omega 1}=0.55,\quad C_{\omega 2}=0.075 \qquad (9)$$

and

$$f_\omega=\frac{0.1+10R_t/20}{1+10R_t/20} \qquad ;R_t=\frac{k}{\upsilon\omega} \qquad (10)$$

The Wilcox K-ω models use a slightly different nomenclature for both coefficients and Schmidt numbers, than shown above; here however, for clarity, a more general nomenclature is used. The Wilcox nomenclature (α,β) is also noted above. The production term P_k is as follow:

$$P_k=-\overline{u_i'u_j'}\frac{\partial U_i}{\partial x_j}\approx \upsilon_t\left(\frac{\partial U_i}{\partial x_j}+\frac{\partial U_j}{\partial x_i}\right)\frac{\partial U_i}{\partial x_j} \qquad (11)$$

The difference between the ω equation of the few K-ω models is restricted to, as in the case of the ε equation the values of the Schmidt number (σ_ω), coefficients and damping functions. There is however, an additional (unnecessary) complexity connected to K-ω models which is the definition of ω. There exist two different versions:

$$\omega \equiv \frac{\varepsilon}{k} \qquad \upsilon_t = \frac{k}{\omega} \qquad (12)$$
$$\omega \equiv \frac{\varepsilon}{\beta^* k} \qquad (\beta^* = 0.09)$$

In regions of low turbulence where both k and ε go to zero, large numerical problems for K- ε model appear in the ε equation as k becomes zero. On the contrary, no such problems appear in the ω equation. One of the applications of k-ω model is used to predict transitional, recirculation flow.

2.2.3 The Spalart-Allmaras model

The Spalart-Allmaras model is a relatively simple one-equation model that solves a modeled transport equation for the kinematic eddy (turbulent) viscosity. This embodies a relatively new class of one-equation models in which it is not necessary to calculate a length scale related to the local shear layer thickness. The transported variable in the Spalart-Allmaras model, $\tilde{\upsilon}$, is identical to the turbulent kinematic viscosity except in the near-wall (viscous-affected) region. The transport equation for $\tilde{\upsilon}$ is,[14]:

$$\frac{\partial}{\partial t}(\rho\tilde{\upsilon}) + \frac{\partial}{\partial x_i}(\rho\tilde{\upsilon}u_i) = G_\upsilon + \frac{1}{\sigma_{\tilde{\upsilon}}}\left[\frac{\partial}{\partial x_j}\left\{(\mu + \rho\tilde{\upsilon})\frac{\partial\tilde{\upsilon}}{\partial x_j}\right\} + C_{b2}\rho\left(\frac{\partial\tilde{\upsilon}}{\partial x_j}\right)^2\right] - Y_\upsilon + S_{\tilde{\upsilon}} \qquad (14)$$

where G_υ is the production of turbulent viscosity and Y_υ is the destruction of turbulent viscosity that occurs in the near-wall region due to wall blocking and viscous damping. $\sigma_{\tilde{\upsilon}}$ and C_{b2} are constants and υ is the molecular kinematic viscosity. $S_{\tilde{\upsilon}}$ is a user-defined source term.

The production term G_υ is defined as:

$$G_\upsilon = C_{b1}\rho\tilde{S}\tilde{\upsilon} \qquad ;C_{b1} = 0.1355 \qquad (15)$$

$$\tilde{S} = S + \frac{\tilde{\upsilon}}{\kappa^2 d^2} f_{\upsilon 2} \qquad ;\kappa = 04187 \qquad (16)$$

$$f_{\upsilon 2} = 1 - \frac{\chi}{1 + \chi f_{\upsilon 1}} \quad ; \quad \left(\chi = \frac{\tilde{\upsilon}}{\upsilon}\right) \quad ; \quad f_{\upsilon 1} = \frac{\chi^3}{\chi^3 + C_{\upsilon 1}^3} \quad ;C_{\upsilon 1} = 7.1 \qquad (17)$$

d is distance from the wall and S is a scalar measure of the deformation tensor and is based on the magnitude of the vorticity :

$$S = \sqrt{2\Omega_{ij}\Omega_{ij}} \qquad (18)$$

Where Ω_{ij} is the mean rate of rotation tensor and is defined by:

$$\Omega_{ij} = \frac{1}{2}\left(\frac{\partial u_i}{\partial x_j} - \frac{\partial u_j}{\partial x_i}\right) \qquad (19)$$

The destruction term Y_υ is defined as:

$$Y_\upsilon = C_{\omega 1}\rho f_\omega \left(\frac{\tilde{\upsilon}}{d}\right)^2 \qquad ;C_{\omega 1} = 2.435 \qquad (20)$$

where

$$f_\omega = g\left[\frac{1 + C_{\omega 3}^6}{[r + C_{\omega 2}(r^6 - r)]^6 + C_{\omega 3}^6}\right] \qquad ;C_{\omega 2} = 0.3 \quad ;C_{\omega 3} = 2.0 \qquad (21)$$
$$r = \frac{\tilde{\upsilon}}{\tilde{S}\kappa^2 d^2}$$

The Spalart-Allmaras model was designed specifically for aerospace applications involving wall-bounded flows and has been shown to give good results for boundary layers subjected to adverse pressure gradients. It is also gaining popularity for turbo machinery applications.

3 RESULTS AND DISCUSSION

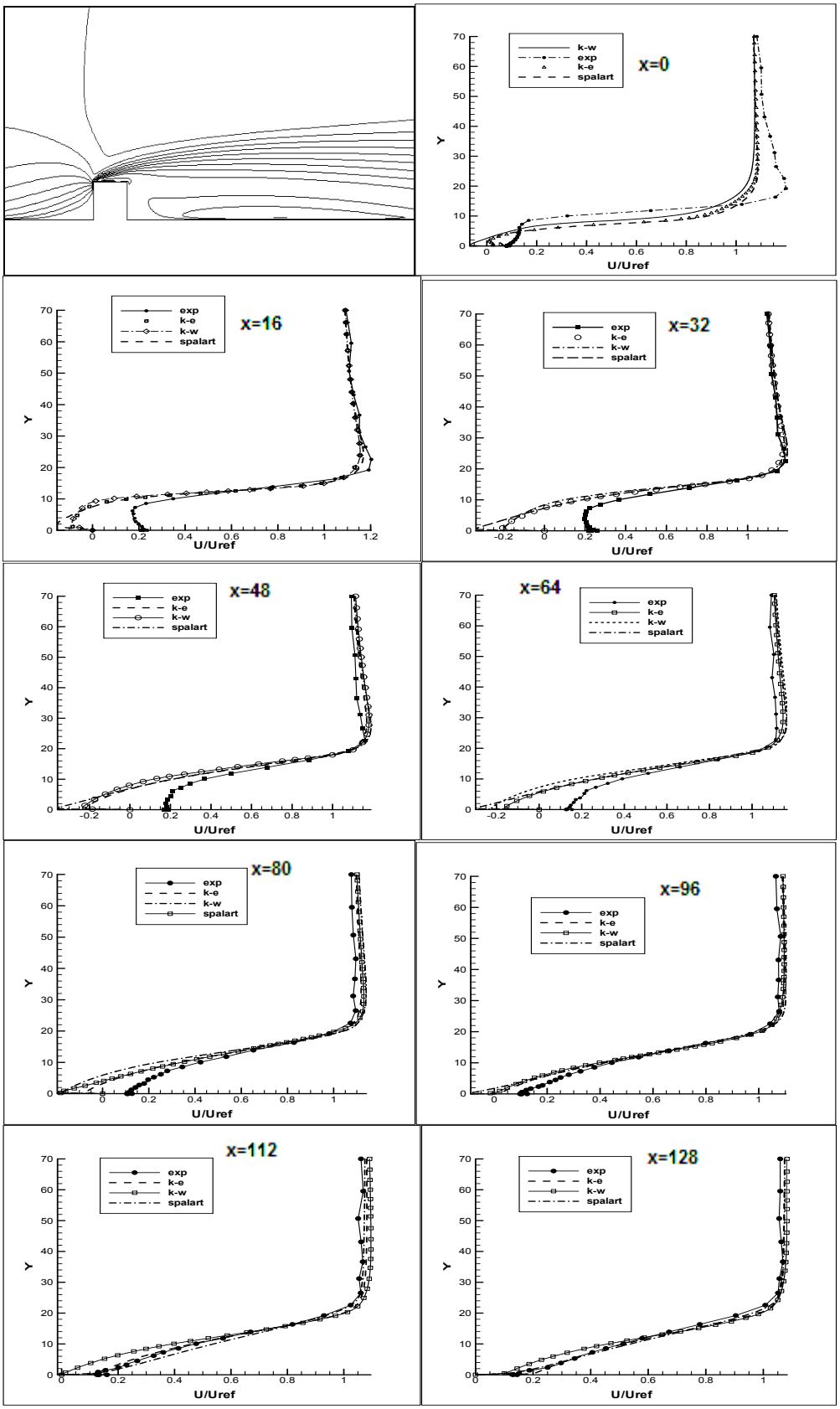

Figure 4: Step1, Obstacle impacted on flat plate

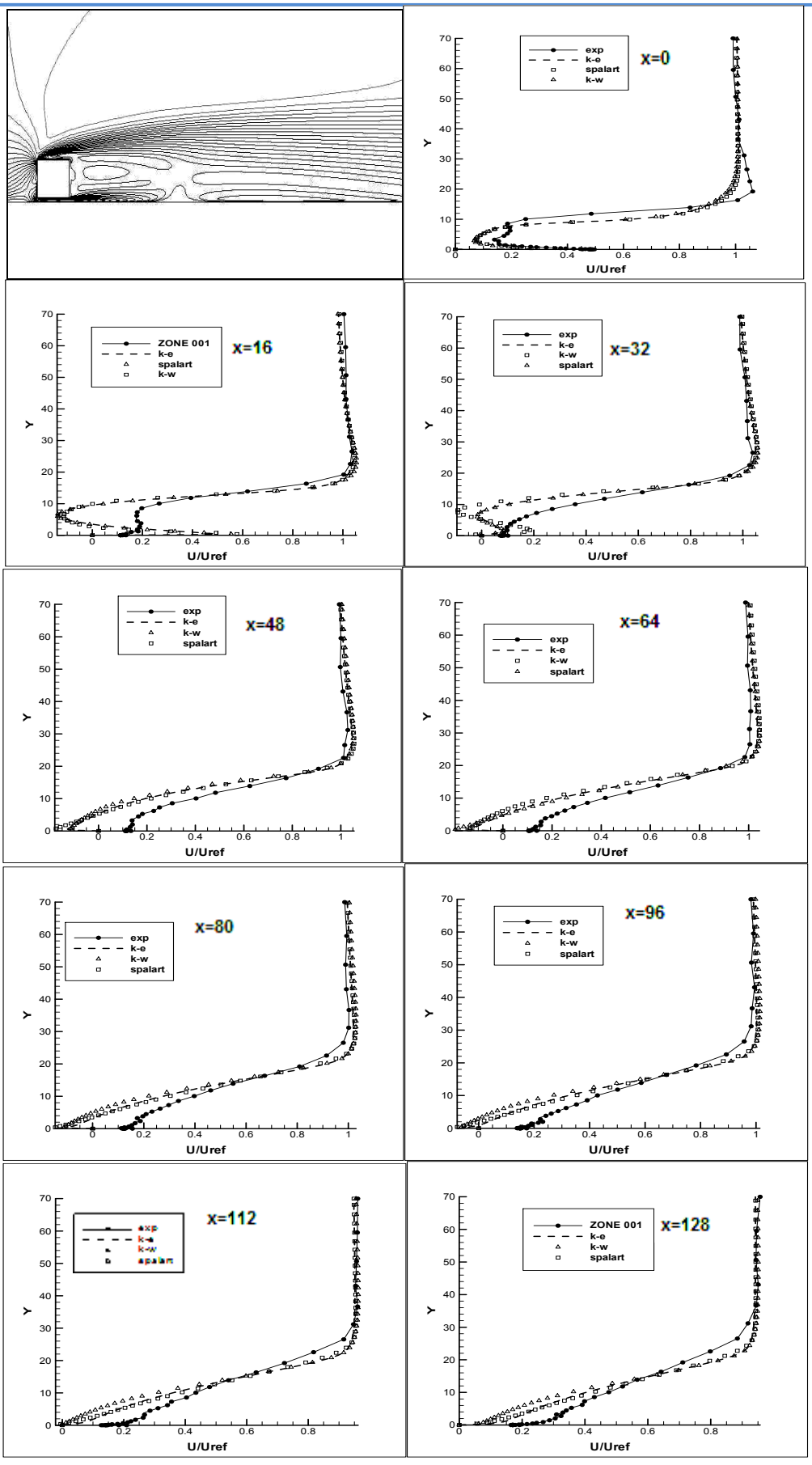

Figure 5: Step2, 1mm distance from flat plate

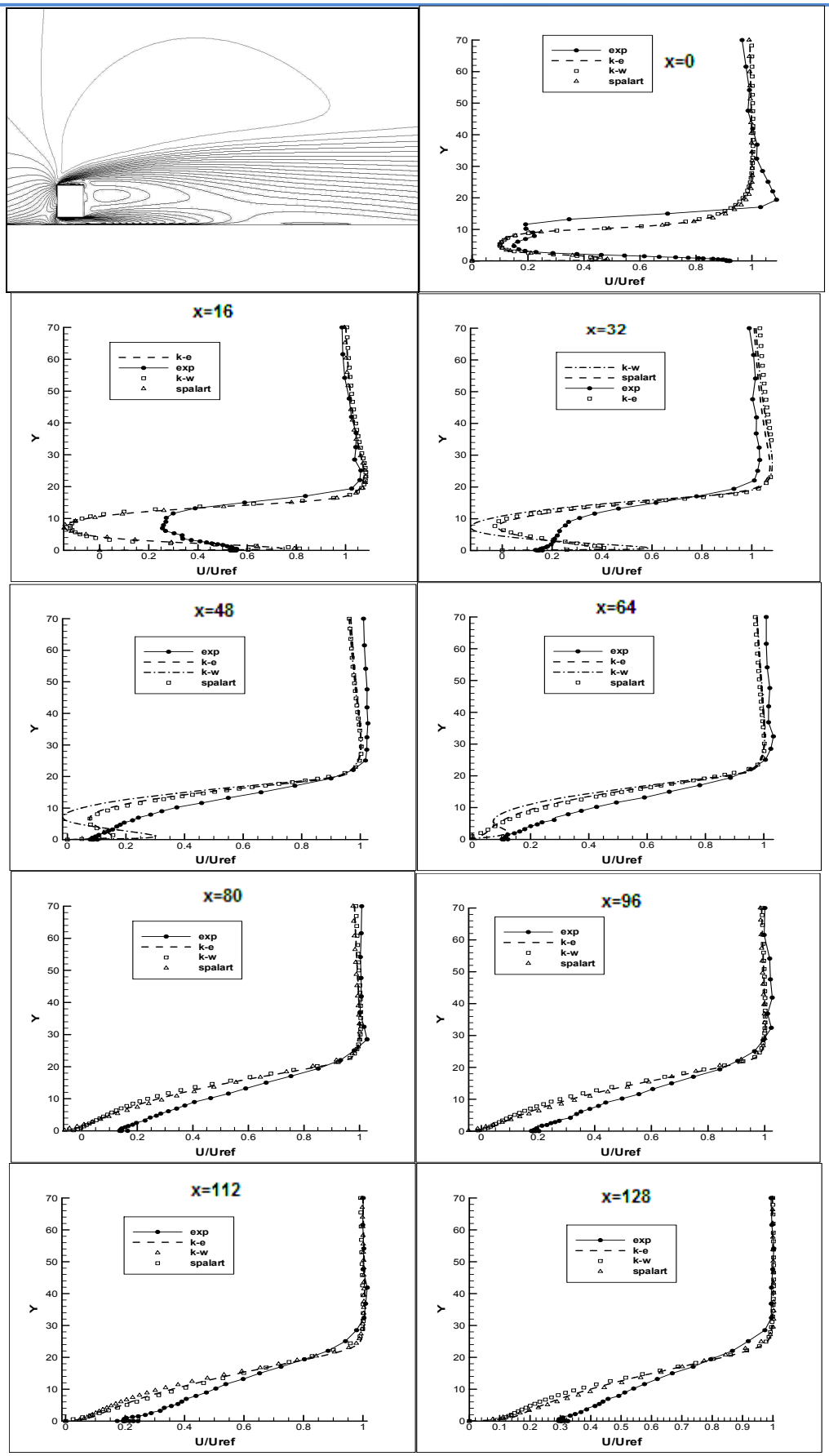

Figure 6: Step3, 2mm distance from flat plate

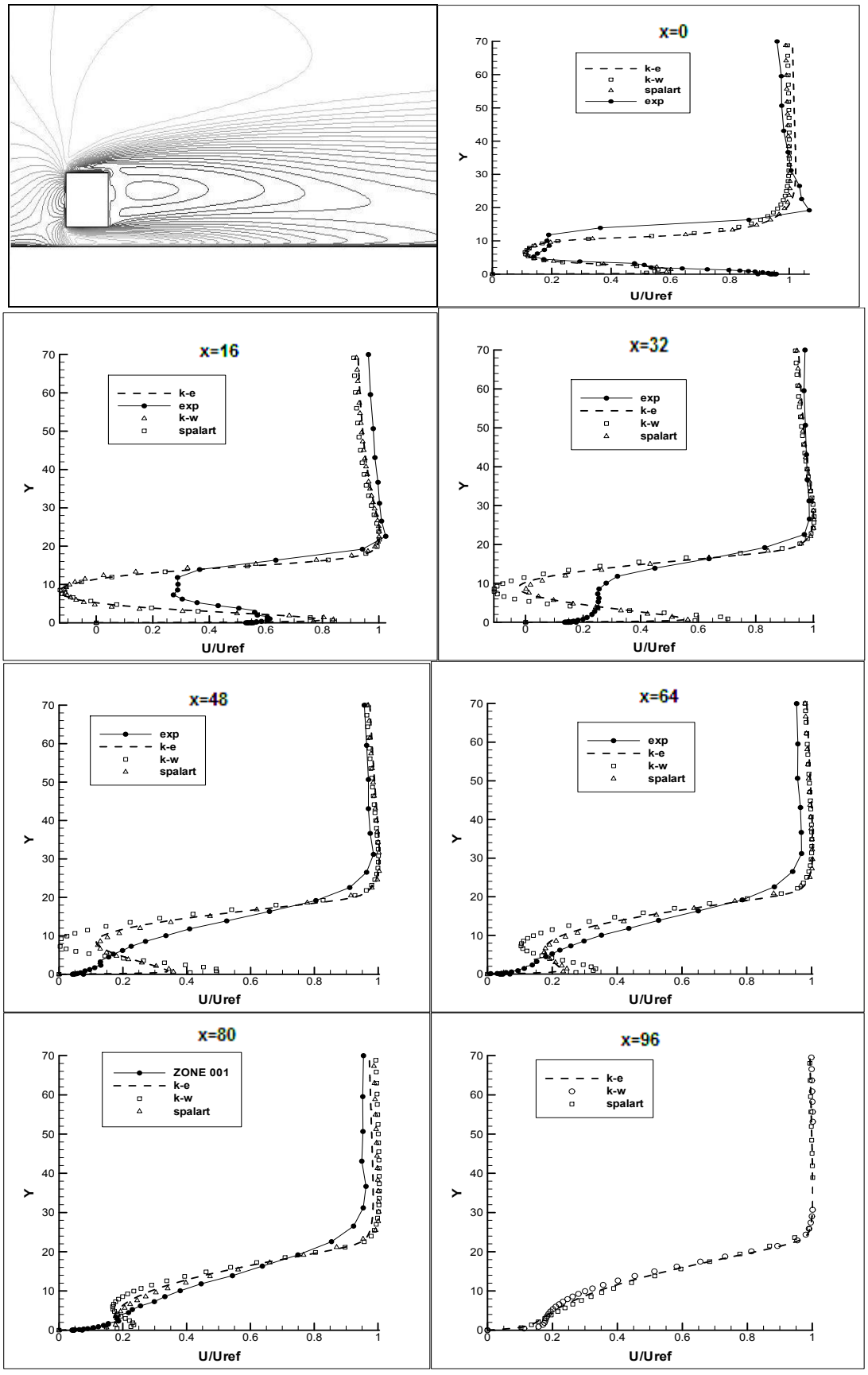

Figure 7: Step4, 3mm distance from flat plate

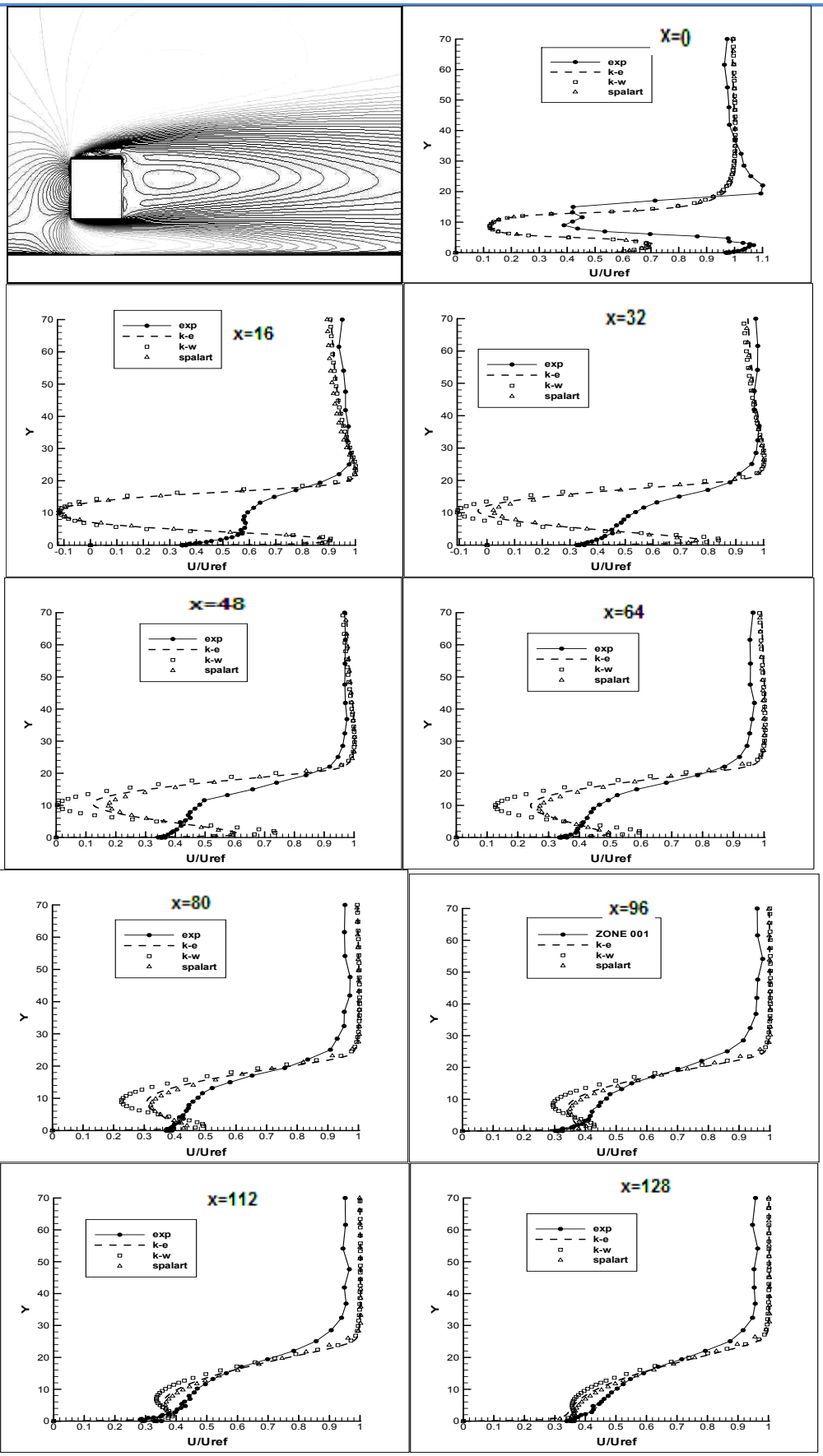

Figure 8: Step5, 5mm distance from flat plate

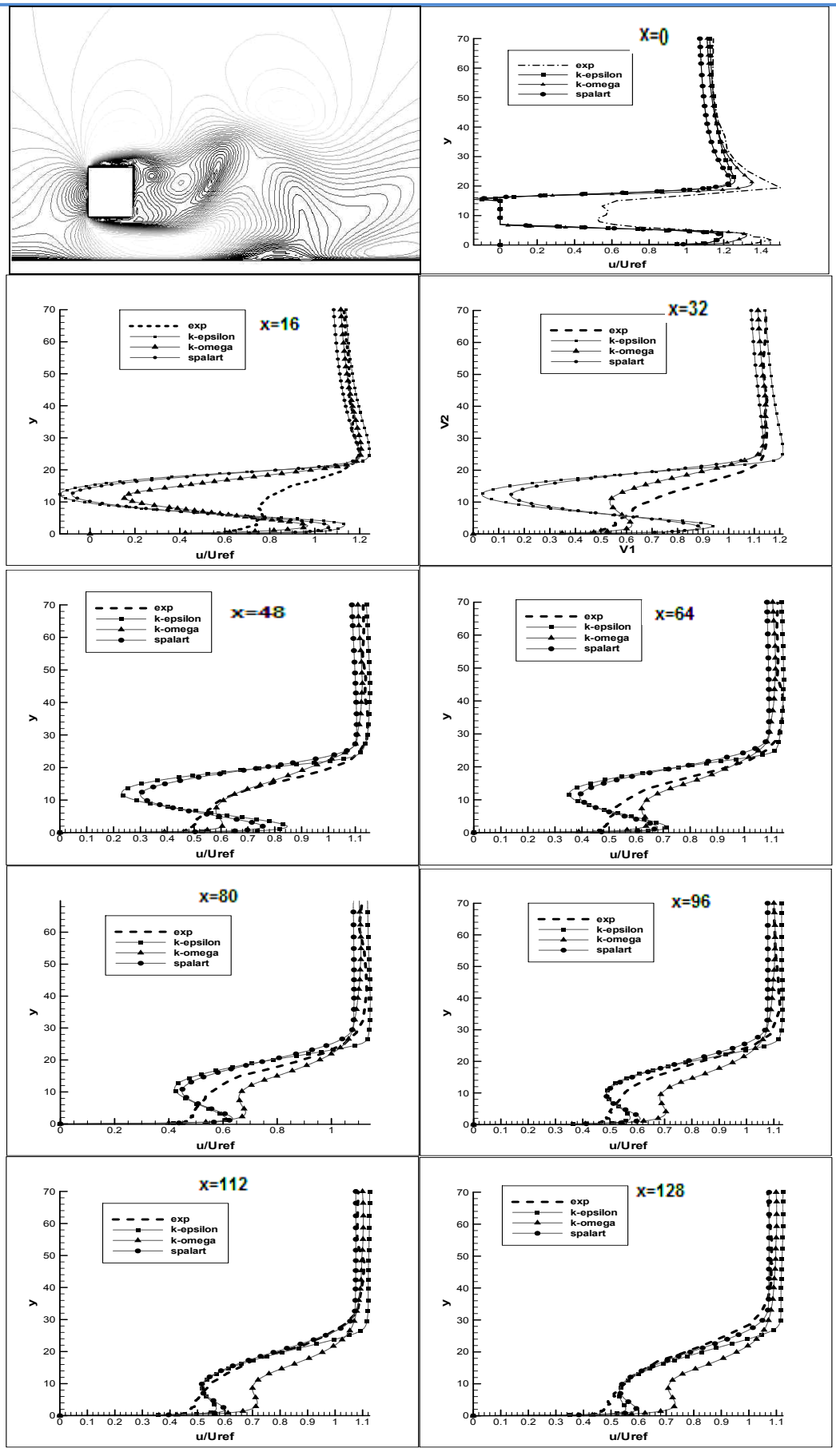

Figure 9: Step6, 7mm distance from flat plate

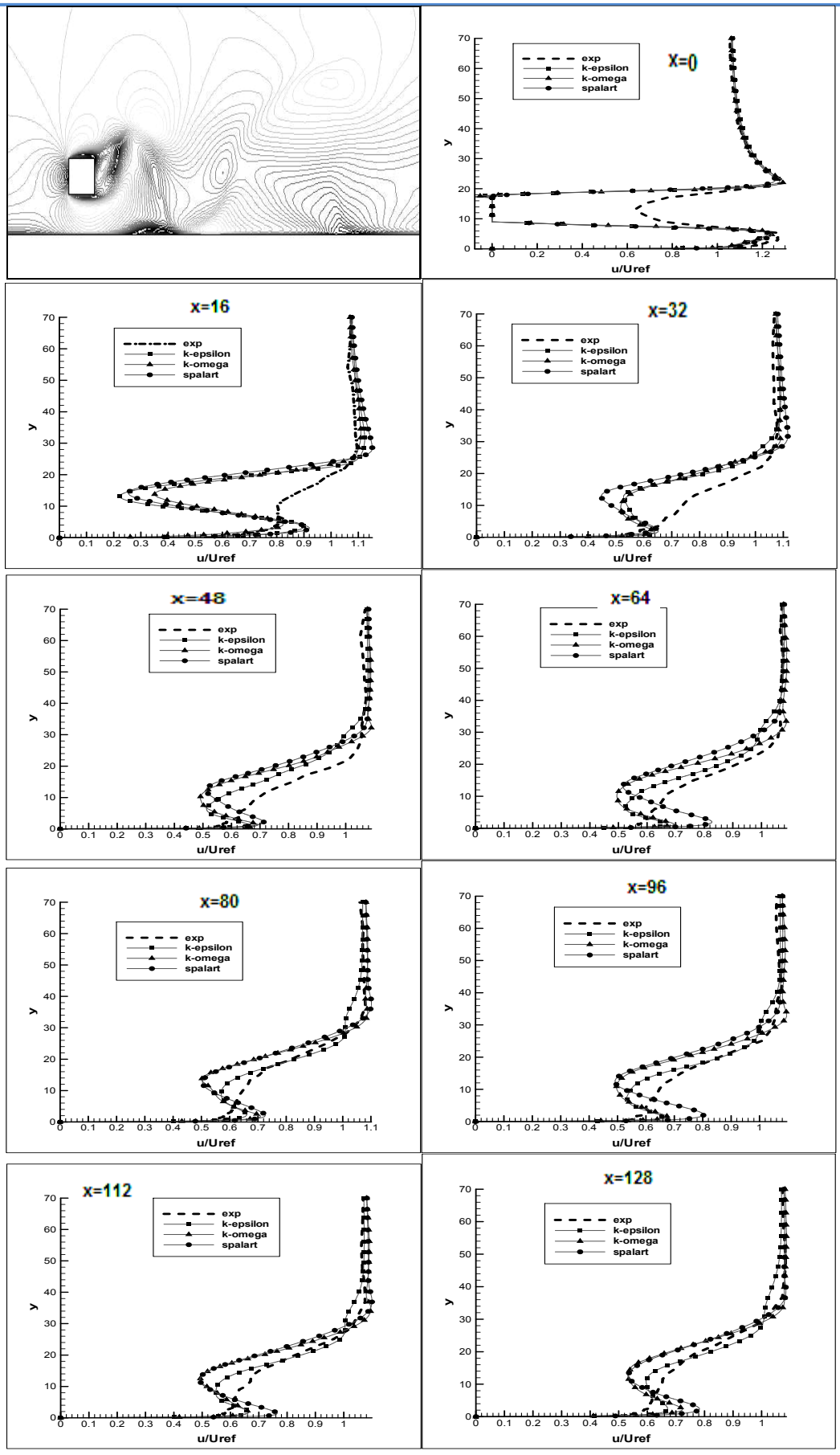

Figure 10: Step7, 9mm distance from flat plate

CONCLUSIONS

The uniform shear flow past a square cylinder placed near a plane wall has been investigated numerically for Reynolds number up to 11000 and at different values of cylinder to wall gap height. The wall causes a difference in strength between two vortex rows. Downstream of the cylinder the boundary layer belong the wall separates in the vicinity of the vortex formation region and a recirculation region forms on the wall at all Reynolds number. The recirculation zone on the wall is transported downstream with time without detaching from the wall. It has been found that the strength of the positive vortices arising from the lower side of the cylinder reduces with the decrease of gap height.
When the cylinder is close proximity to the wall, a single row of counter clockwise vortices forms in the wake. We found that the vortex shedding is suppressed at a critical gap height and the gap height depends on Re. At the gap height when vortex shedding is suppressed the shear layer which is separated from the lower side of the cylinder attaches on the cylinder itself. The average drag coefficient on the cylinder decreases with the reduction of gap height. Cylinder experiences a large positive lift when brought close to the wall (fig.4 to 10).
In fig.4 to 10 for x=0 to 32 in upper layers experimental and numerical results are similar but in the layers close to the wall just concavity and convexity of velocity profile are the same. By receding from cylinder in fig.4 to 10 for x=48 to 128 in the layers close to the wall also experimental and numerical results come close to each other.
At the gap height 7mm and 9mm (fig.9 and 10) the oscillatory solutions due to the existence of vortices were noticed. To gain the averaged values of the velocity, as is the case for hot wire measurements as well, averaging of the velocities over a period of oscillation was employed. In this case we have oscillating lift coefficient by means of periodic vortexes. K-ω model's results are closer to experimental data in these two steps.
In fig.4 to 10 for x=0 to 32 there are three points in which $\partial u / \partial y = 0$. This case occurs by two parts: the lower part washes away the thin remaining boundary layer on the plat away, while the second part of the flow jumps upon the top side of the insert, forming the wake zone at the downstream to the obstacle.

REFERENCES

[1] S. Bhattacharyya, D.K. Maiti , Shear flow past a square cylinder near a wall, Department of Mathematics, Indian Institute of Technology, Kharagpur 721302, India Received 29 January 2004; accepted 12 April 2004 Available online 28 September 2004

[2] Necati Mahir , Three-dimensional flow around a square cylinder near a wall, Eskisehir Osmangazi University, School of Engineering and Architecture, Mechanical Engineering Department, 26480 Bat Meselik, Eskisehir, Turkey Accepted 5 January 2009

[3] R.W. Davis, E.F. Moore, A numerical study of vortex shedding from rectangles, J. Fluid Mech. 116 (1982) 475–506.

[4] R. Franke, W. Rodi, Numerical calculation of laminar vortex shedding flow past cylinders, J. Wind Eng. Ind.Aerodyn. 35 (1990) 237–257.

[5] A. Okajima, H. Sakai, Numerical simulation of laminar and turbulent flow around rectangular cylinders, Int. J.Numer. Meth. Fluids 15 (1992) 999–1012.

[6] S.V. Patankar, K.M. Kelkar, Numerical prediction of vortex shedding behind a square cylinder, Int. J. Numer.Meth. Fluids 14 (1992) 327–341.

[7] S.Sarkar,SudiptoSarkar, Vortex dynamics of a cylinder wake in proximity to a wall, Department of Mechanical Engineering, Indian Institute of Technology Kanpur, Kanpur 208016, India Accepted 13 August 2009

[8] Lars Davidson , An Introduction to Turbulence Models , Department of Thermo and Fluid Dynamics ,Chalmer University of Technology, 2003

[9] K. Hanjali´c , Closure Models for Incompressible Turbulent Flows , Department of Applied Physics Delft University of Technology Lorentzweg 1, 2628 CJ Delft, The Netherlands

[10] Jonas Bredberg ,On Two-equation Eddy-Viscosity Models, Department of Thermo and Fluid Dynamics CHALMERS UNIVERSITY OF TECHNOLOGY, Goteborg Sweden 2001

[11] D. Choudhury, Introduction to the Renormalization Group Method and Turbulence Modeling,
Fluent Inc. Technical Memorandum TM-107, 1993

[12] F. R. Menter, M. Kuntz, and R. Langtry, Ten Years of Experience with the SST Turbulence Model, In K. Hanjalic, Y. Nagano, and M. Tummers, editors, *Turbulence, Heat and Mass Transfer 4*, pages 25-632. Begell House Inc., 2003.

[13] G. I. Barenblatt, A. J. Chorin, and V. M. Prostokishin , The turbulent wall jet: A triple-layered structure and incomplete similarity

[14] P. Spalart and S. Allmaras, A one-equation turbulence model for aerodynamic flows, Technical Report AIAA-92-0439, American Institute of Aeronautics and Astronautics, 1992.

[15] D. Ahlman, G.Brethouwer, and A.V. Johansson, Direct numerical simulation of a plane turbulent wall-jet including scalar mixing, Linné Flow Centre, Department of Mechanics, Royal Institute of Technology, SE-100 44 Stockholm, Sweden 2007

[16] A. A. Adeniji-Fhshola and C. P. Chen, INLET TURBULENCE INTENSITY LEVEL AND CROSS-STREAM DISTRIBUTION EFFECTS ON THE HEAT TRANSFER IN PLANE WALL JETS, Int. Comm. Heat Mass Transfer Vol. 16, pp. 833-842, 1989

[17] G. Bosch, W. Rodi, Simulation of vortex shedding past a square cylinder near a wall, Int. J. Heat Fluid Flow 17(1996) 267–275.

[18] G. Bosch, M. Kappler, W. Rodi, Experiments on the flow past a square cylinder placed near a wall, Exp. Therm. Fluid Sci. 13 (1996) 292–305.

[19] T. Liou, S. Chen, P. Hwang, Large eddy simulation of turbulent wake behind a square cylinder with a nearby wall, J. Fluid Eng. 124 (2002) 81–90.